Collective intersubband spin-density excitations in a quantum wire in a magnetic field

1998 J. Phys.: Condens. Matter 10 4267

(http://iopscience.iop.org/0953-8984/10/19/014)

J. Phys.: Condens. Matter **10** (1998) 4267–4279. Printed in the UK PII: S0953-8984(98)89946-3

Collective intersubband spin-density excitations in a quantum wire in a magnetic field

Arne Brataas†¶, Vidar Gudmundsson‡, A G Mal'shukov§ and K A Chao†‖

† Department of Physics, Norwegian University of Science and Technology, N-7034 Trondheim, Norway

‡ Science Institute, University of Iceland, Dunhaga 3, IS-107 Reykjavik, Iceland

§ Institute of Spectroscopy, Russian Academy of Sciences, 142092 Troitsk, Moscow Region, Russia

‖ Department of Theoretical Physics, Lund University, S-223 26 Lund, Sweden

Received 11 December 1997

Abstract. We study an interacting electron gas parabolically confined to a quantum wire in a perpendicular magnetic field. We consider the case of more than one subband occupied in the ground state. The intersubband spin-density excitations are calculated within the Hartree–Fock random-phase approximation. Similarly to the case in the absence of a magnetic field, vertex corrections to the electron spin polarizability are important, leading to collective spin-density excitations red-shifted with respect to the Hartree–Fock single-particle energies. In a finite magnetic field, the triplet of spin-density excitations splits. The splitting is at its maximum if the chemical potential is in between the bottom of a spin-up subband and the bottom of a spin-down subband, when the g-factor is greatly enhanced due to the exchange interaction.

1. Introduction

Low-dimensional interacting electron systems in a magnetic field have attracted substantial interest in recent years. Quasi-one-dimensional systems, quantum wires, can be produced by using gate voltages to confine the electron gas starting from a semiconductor quantum well. In these systems the electrons are free to move in only one direction and are localized in the others. These systems display a variety of interesting physical effects, some of which can be explored by optical measurements. The spin-density and charge-density excitations of low-dimensional systems can be measured by means of inelastic light scattering [1] and the charge-density excitations also contribute to the far-infrared absorption. A variety of calculations of the intra- and intersubband charge-density excitations in quantum wires have been performed on the basis of the Hartree random-phase approximation (H-RPA) [2–8], and these are found to agree well with experiment [9–14]. Beyond the H-RPA, Yang and Aers [15] have used a Hartree–Fock random-phase approximation (HF-RPA) to find a roton minimum in the intrasubband magnetoplasmon dispersion, whose existence was experimentally confirmed in reference [13]. In that experiment [13], intersubband spin-flip excitations were also observed. Recently, spin excitations in coupled double layers in a perpendicular magnetic field were also studied [16]. Tanatar has investigated the spin-density excitation spectra in the extreme quantum limit when only one subband is occupied [17].

¶ Present address: Laboratory of Applied Physics and Delft Institute of Microelectronics and Submicrontechnology (DIMES), Delft University of Technology, Lorentzweg 1, 2628 CJ Delft, The Netherlands.

0953-8984/98/194267+13$19.50

For intrasubband and intersubband spin-density excitations in quantum wires, we have recently shown [18, 19] that, for zero magnetic field, vertex corrections to the electron spin polarizability are important. They lead to collective spin-density excitations with resonance energies considerably red-shifted with respect to the single-particle Hartree–Fock energies. For the charge-density excitation spectra, vertex corrections are less important. However, in our previous works [18, 19], the effect of a finite magnetic field on the spin-density excitations was not considered.

For a two-dimensional electron gas (2DEG) in a perpendicular magnetic field, Longo and Kallin [20] have calculated the spin-density excitations in the HF-RPA and by using the generalized single-mode approximation [21, 22]. They showed that the HF-RPA produces good results for integer filling factors, but is less satisfactory for fractional fillings because important correlations are neglected in this case. Nevertheless, the HF-RPA still serves to give qualitative results [20], and can serve as a benchmark for theories including correlation effects.

Many problems in accounting for electron–electron interactions in 2D systems are associated with the macroscopic degeneracy of the Landau levels. Unlike in 2D systems, in one-dimensional systems the Landau levels are non-degenerate. However, in one-dimensional systems strong correlations usually take place even for weakly interacting particles [23–28]. The system that we will study, a quantum wire with more than one subband occupied, is in the intermediate regime between the 2DEG and the one-dimensional cases. We expect the one-dimensional correlations to be weaker in the case of several occupied subbands. They are also less important for intersubband excitations as well as for intrasubband excitations whose energy is not very low. We will therefore use the HF-RPA to calculate the different intersubband spin-density excitations of the electron gas in a perpendicular magnetic field $\boldsymbol{B}$. Within this scheme, first, the ground state is calculated to find the Hartree–Fock single-particle states and energies. Second, the Hartree–Fock single-particle states and energies are used to derive the excitation energies in the corresponding time-dependent equation, where the recombination between the electrons and holes (bubble diagrams) and the interaction between the excited electrons and holes (ladder diagrams) are taken into account.

In order to make the description more explicit, let us consider a GaAs quantum wire with a parabolic confinement potential of a characteristic frequency ω_0. The eigenstates in the wire are specified by the quantum numbers n for the subband, k for the longitudinal momentum, and $\sigma = \pm 1$ for the spin. An intersubband electron–hole excitation is created by promoting an electron from the initial state (n', k, σ') to the final state (n, k, σ). In the absence of electron–electron interaction, the intersubband electron–hole pair has the excitation energy

$$E_{k,\Delta\sigma} = (n - n')\overline{h}\Omega + \Delta\sigma\,\overline{h}\omega_Z/2$$

expressed in terms of the spin difference $\Delta\sigma = \sigma - \sigma'$, the effective subband separation $\overline{h}\Omega = \overline{h}(\omega_0^2 + \omega_c^2)^{1/2}$, and the Zeeman energy splitting $\overline{h}\omega_Z = g\mu_B B$. Here ω_c is the cyclotron frequency, g is the Landé g-factor in GaAs, and μ_B is the Bohr magneton. The non-interacting intersubband spin-density excitation energies are independent of the longitudinal quantum number k, and will thus give a sharp peak in the spectra at energies equal to $(n - n')\overline{h}\Omega + \Delta\sigma\,\overline{h}\omega_Z/2$. In the dipole limit that we will consider, only transitions with $|n - n'| = 1$ are allowed.

In the Hartree approximation in the ground state, the screening of the external parabolic potential reduces the single-particle subband separation from $(n - n')\overline{h}\Omega$ to a smaller k-dependent subband separation $\Delta^H_{nn'k}$. There is no interaction between an electron and a hole

with opposite spin in the excited states, so the spin-flip excitation energies are given by

$$E^H_{k,\Delta\sigma} = \Delta^H_{nn'k} + \Delta\sigma\,\bar{h}\omega_Z/2$$

in the Hartree random-phase approximation. In this case, the intersubband spin-density excitation energies are lowered with respect to the non-interacting case. Furthermore, its dependence on the longitudinal quantum number k results in a broader peak centred around a mean intersubband excitation energy. However, the energy difference between the three different spin-flip excitations ($\Delta\sigma = 2$, $\Delta\sigma = 0$, and $\Delta\sigma = -2$) is completely determined by the Zeeman terms

$$\Delta E^H_{k,+} = E^H_{k,2} - E^H_{k,0} = \bar{h}\omega_Z \qquad \text{and} \qquad \Delta E^H_{k,-} = E^H_{k,-2} - E^H_{k,0} = -\bar{h}\omega_Z$$

as for non-interacting electrons.

In the Hartree–Fock approximation of the ground state, the effective Zeeman energy splitting, $g^k_n\bar{h}\omega_Z$, for the self-consistent single-particle states can be enhanced from $\bar{h}\omega_Z$ due to the exchange interaction, which favours unequal occupation of the spins. The enhancement of the g-factor depends on the electronic density, the magnetic field, the subband index, and the longitudinal momentum. It has a maximum value when the chemical potential is close to a subband energy, and a minimum value when the chemical potential is in between two subband energies [29–32]. The screening of the external potential causing a smaller subband separation $\Delta^{HF}_{nn'k}$ is similar to the results of the Hartree approximation. Excluding vertex corrections for the excited states, the spin-dependent energy is

$$E^{HF,0}_{k,\Delta\sigma} = \Delta^{HF}_{nn'k} + (\sigma g^k_n - \sigma' g^k_{n'})\bar{h}\omega_Z/2.$$

Within this approximation the difference in the spin-flip excitation energies

$$E^{HF,0}_{k,2} - E^{HF,0}_{k,-2} = (g^k_n + g^k_{n'})\bar{h}\omega_Z$$

is thus larger than its corresponding non-interacting value. For the long-wavelength charge-density excitations, the magnetoplasmons, the excitation energies are increased with respect to the single-particle excitation energies due to the depolarization shift (bubble diagrams). There are no modes corresponding to the magnetoplasmon for the spin-flip excitations ($\Delta\sigma = \pm 2$), since an electron and a hole with opposite spin cannot recombine. The vertex correction (ladder diagrams) for the excited states lowers the spin-flip excitation energies relative to the intersubband Hartree–Fock single-particle energies, and also gives the excitations a collective character forming a narrow excitation energy band. The spin-flip excitation energy is typically

$$(E^{HF}_{k,\Delta\sigma})^2 = (E^{HF,0}_{k,\Delta\sigma})^2 - (V_{k\Delta,\sigma})^2$$

in the Hartree–Fock random-phase approximation, where $V_{k,\Delta\sigma}$ is a measure of the vertex corrections. Thus, the difference in the spin-flip energies, $\Delta E^{HF}_k = E^{HF}_{k,2} - E^{HF}_{k,-2}$, generally does not simply reflect the enhanced Landé factor which is a single-particle parameter, but also accounts for collective effects.

It is the purpose of this paper to consider the spin-density excitations in a quantum wire in a magnetic field that can be measured experimentally and to further study the relation between the enhancement of the g-factor and the intensity and the excitation energies of the different spin-density excitation components.

In the next section, the model Hamiltonian for the electrons in the quantum wires is introduced and the Hartree–Fock random-phase approximation for the ground state and excited states is described. The numerical results are discussed in section 3 and finally we make some concluding remarks in section 4.

2. Model

We start with a strictly two-dimensional electron gas extended in the xy-plane but restricted in the z-direction. The motion in the z-direction is disregarded, since the electrons are confined to the lowest subband under the low-temperature experimental conditions. A transverse potential $V(y)$ is imposed on the electron system. Along the longitudinal direction, which is parallel to the x-axis, the quantum wire has a finite length L, and there is a static magnetic field, $\boldsymbol{B} = \boldsymbol{\nabla} \times \boldsymbol{A}(\boldsymbol{r})$ applied in the z-direction. The electrons interact through the Coulomb interaction $V(|\boldsymbol{r} - \boldsymbol{r}'|) = e^2/(\kappa|\boldsymbol{r} - \boldsymbol{r}'|)$, where κ is the dielectric constant of the surrounding medium. The Zeeman energy is $g\mu_B\sigma B_z/2$, where the spin is $\sigma = \pm 1$ and $g = -0.44$ is the Landé g-factor for GaAs. We use the Landau gauge $\boldsymbol{A}(\boldsymbol{r}) = (-By, 0)$, and define the magnetic length $l_c = [\hbar/(m\omega_c)]^{1/2}$. The Hartree–Fock calculation scheme is well known for calculating the electronic excitations [29–32, 18, 19]. For completeness in discussing our numerical results, we outline the method below.

2.1. The ground state

We assume periodic boundary conditions in the longitudinal direction, so that the single-particle wave-functions have the form

$$\Psi(x, y) = L^{-1/2} \exp(\mathrm{i}kx)\psi_{nk}(y)$$

where the longitudinal wave-vector $k = (2\pi/L) \times$ integer. We define the non-interacting transverse Hamiltonian

$$H_0(y) = -\frac{\hbar^2}{2m}\left(\frac{\mathrm{d}^2}{\mathrm{d}y^2} - k^2 + \frac{2k}{l_c^2}y\right) + \frac{1}{2}m\omega_c^2 y^2 + \frac{1}{2}g\mu_B\sigma B + V(y) \tag{1}$$

and the Hartree potential

$$V_H(y) = \frac{2e^2}{\kappa L}\sum_{nk\sigma} f_{nk\sigma}\int_{-\infty}^{\infty}\mathrm{d}y\ \ln|y - y'||\phi_{nk\sigma}(y)|^2 \tag{2}$$

and also the non-local Fock operator

$$V_F^{k\sigma}(y', y) = -\frac{2e^2}{\kappa L}\sum_{n'k'} f_{n'k'\sigma}K_0(|k - k'||y - y'|)\phi_{nk\sigma}(y')\phi_{nk\sigma}(y) \tag{3}$$

where $K_0(x)$ is the modified Bessel function. The transverse wave-functions, $\phi_{nk\sigma}$, are determined self-consistently by the equation

$$[H_0(y) + V_H(y)]\phi_{nk\sigma}(y) + \int \mathrm{d}y'\ V_F^{k\sigma}(y', y)\phi_{nk\sigma}(y') = \epsilon_{nk\sigma}\phi_{nk\sigma}(y). \tag{4}$$

We will study the quantum wire with a parabolic potential $V(y) = m\omega_0^2 y^2/2$ which is a good description for electrostatically defined wires [33]. The Hartree–Fock equation (4) has been solved numerically by discretizing the transverse coordinate with a high-order numerical method and then solving the differential–integral equation. This direct numerical method generally gives better convergence than the method that we have used previously [18, 19, 34], where the Hartree–Fock single-particle states were expanded in the basis of the non-interacting states. The improvement is of significance when the Hartree–Fock wave-function differs strongly from the non-interacting solution. As usual the self-consistent Hartree–Fock equation is solved by iteration.

2.2. Excited states

The charge-density excitations can be measured in far-infrared absorption or in Raman scattering when the polarizations of the incoming and scattered photons are parallel to each other. The spin-density excitations can be measured in Raman scattering if the two polarizations of the incoming and scattered light are perpendicular to each other [35]. The charge-density excitations and spin-density excitations are given by the imaginary parts of the charge–charge and the three possible spin–spin correlation functions. These correlation functions are written as

$$\chi_A(\omega) = -\frac{\mathrm{i}}{\hbar}\int_0^\infty \mathrm{d}t\ \mathrm{e}^{\omega t}\langle|[\hat{A}(t), \hat{A}^\dagger(0)]|\rangle \tag{5}$$

where $\hat{A}$ can be the charge-density operator $\hat{\rho}(\boldsymbol{q}, t)$, the spin-density operator $\hat{\sigma}_z(\boldsymbol{q}, t)$ along the spin-quantization axis, or the spin-flip operators, $\hat{\sigma}_\pm(\boldsymbol{q}) = \hat{\sigma}_x(\boldsymbol{q}) \pm \mathrm{i}\hat{\sigma}_y(\boldsymbol{q})$. Here $\langle|\cdots|\rangle$ denotes the thermodynamic average. Since $\hat{\rho}^\dagger(\boldsymbol{q}, t) = \hat{\rho}(-\boldsymbol{q}, t)$, $\hat{\sigma}_z^\dagger(\boldsymbol{q}, t) = \hat{\sigma}_z(-\boldsymbol{q}, t)$, and $\hat{\sigma}_+^\dagger(\boldsymbol{q}, t) = \hat{\sigma}_-(-\boldsymbol{q}, t)$ we see that $\chi_\rho^\dagger(\boldsymbol{q}, \omega) = \chi_\rho(-\boldsymbol{q}, -\omega)$, $\chi_{\sigma_z}^\dagger(\boldsymbol{q}, \omega) = \chi_{\sigma_z}(-\boldsymbol{q}, -\omega)$, and $\chi_{\sigma_\pm}^\dagger(\boldsymbol{q}, \omega) = \chi_{\sigma_\mp}(-\boldsymbol{q}, -\omega)$.

We use the Hartree–Fock basis to define the matrix element

$$F_{bs}^{a\sigma}(\boldsymbol{q}) = \int \mathrm{d}\boldsymbol{r}\ \psi_{a\sigma}^*(\boldsymbol{r})\psi_{bs}(\boldsymbol{r})\exp(\mathrm{i}\boldsymbol{q}\cdot\boldsymbol{r}).$$

In the HF-RPA [36, 37, 20, 31, 19] the correlation functions may be expressed as ($A = \rho, \sigma$)

$$\chi_A(\boldsymbol{q}, \omega) = \sum_{cds} s_A K_{cd}^{as}(\boldsymbol{q}, \omega) F_{ds}^{cs}(-\boldsymbol{q}) \tag{6}$$

where $s_\rho = 1$ and $s_\sigma = s$. $K^{\rho s}$ is an induced charge-density matrix and $K^{\sigma s}$ is an induced spin-density matrix satisfying the equation

$$K_{ab}^{As}(\boldsymbol{q}, \omega) = \frac{f_{bs} - f_{as}}{\hbar\omega - (\epsilon_{as} - \epsilon_{bs})}\left[s_A F_{bs}^{as}(-\boldsymbol{q})^* + \sum_{cd\sigma}(V_{c\sigma bs;asd\sigma} - V_{bsc\sigma;asd\sigma})K_{cd}^{As}(\boldsymbol{q}, \omega)\right]. \tag{7}$$

We see that the structure of the eigenvalue problem for the charge-density excitations is the same as for the spin-density excitations, with the only difference lying in the sources $F_{bs}^{as}(-\boldsymbol{q})$, for the charge-density excitations, and $sF_{bs}^{as}(-\boldsymbol{q})$, for the spin-density excitations. In paramagnetic systems at zero magnetic field, the two eigenvalue equations decouple into two separate eigensystems [19], and only the vertex correction enters the eigenequation for the spin-density excitations, because the long-range part of the Coulomb interaction is cancelled out. This is no longer the case with a finite magnetic field, when the occupations of the two spin states are different. The spin-flip correlation function may be expressed as

$$\chi_+(\boldsymbol{q}, \omega) = 4\sum_{cd} K_{cd}^+(\boldsymbol{q}, \omega) F_{d\downarrow}^{c\uparrow}(-\boldsymbol{q}).$$

The induced spin-flip density matrix satisfies

$$K_{ab}^+(\boldsymbol{q}, \omega) = \frac{f_{b\downarrow} - f_{a\uparrow}}{\hbar\omega - (\epsilon_{a\uparrow} - \epsilon_{b\downarrow})}[F_{b\downarrow}^{a\uparrow}(-\boldsymbol{q})^* - \sum_{cd} V_{b\downarrow c\uparrow;a\uparrow d\downarrow} K_{cd}^+(\boldsymbol{q}, \omega)]. \tag{8}$$

Here there is no direct (Hartree) Coulomb interaction between the excited electrons with opposite spins.

3. Numerical results and discussion

We use the intrinsic material parameters $g = -0.44$, $m = 0.067m_0$, and $\kappa = 12.4$ for GaAs in our numerical calculations, where m_0 is the electron mass. The temperature is set at $T = 1.0$ K. The quantum wire has a finite length $L = 1.0$ μm and the external confinement potential strength is $\bar{h}\omega_0 = 5.80$ meV. There are $N = 250$ electrons in the wire, so the one-dimensional electron density is 2.5×10^6 cm^{-1}. We will illustrate the general behaviour of the ground state and the spin-density excitations by showing results of the calculations for magnetic fields of $B = 2.00$ T and $B = 1.75$ T. All of the calculations of the spin-density excitation spectra have been done in the dipole limit, where $\boldsymbol{q} = q\boldsymbol{e}_y$ and $q \to 0$, i.e. we study dipole intersubband excitations.

In the calculation of the ground-state properties, the discrete intervals in the transverse coordinate have been chosen small enough that the error in the Hartree–Fock eigenenergies is less than 0.02 meV. For the excited states, the basis of electron–hole pairs has been made sufficiently large to give an accuracy of the excitation energies within 0.05 meV. The longitudinal f-sum rule is fulfilled to within 2% for all calculations. We have checked that the generalized Kohn theorem [38] is satisfied for the intersubband charge-density excitations, i.e. that there is only a single peak in the dipole intersubband charge-density excitation spectra at an excitation energy $\bar{h}\Omega$.

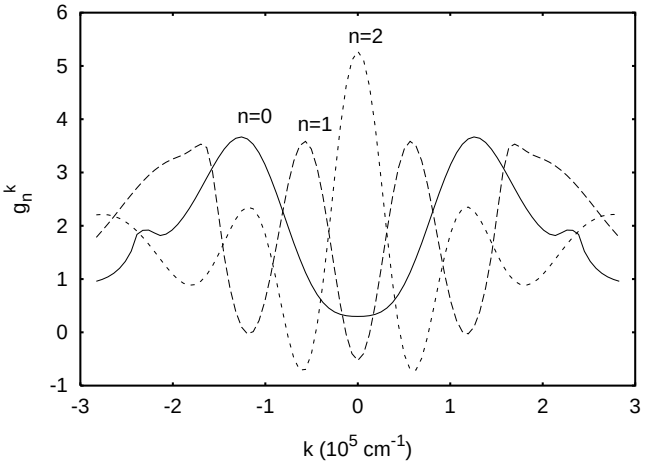

Figure 1. The effective g-factor calculated in the Hartree–Fock approximation for $B = 2.00$ T as a function of the longitudinal momentum. The confinement energy is $\bar{h}\omega_0 = 5.80$ meV, the length of the wire $L_x = 10\,000$ Å, $T = 1.0$ K, $m = 0.067m_0$, $\kappa = 12.4$, and there are $N = 250$ electrons in the wire.

Let us first discuss the case where the magnetic field is $B = 2.00$ T ($l_c = 181$ Å). The effective confinement energy is $\bar{h}\Omega = \bar{h}(\omega_0^2 + \omega_c^2)^{1/2} = 6.75$ meV. In this case there are two subbands occupied both in the Hartree and the Hartree–Fock approximation. The external potential is screened, leading to an effective subband separation that is smaller than the effective external potential strength, $\bar{h}\Omega$. In the Hartree approximation, where the exchange interaction is neglected, the Hartree subband separation is 3.75 meV between subband $n = 0$ and subband $n = 1$, it is 3.89 meV between subband $n = 1$ and subband $n = 2$ and it is 4.00 meV between subband $n = 2$ and subband $n = 3$, all at $k = 0$. The resulting subband separation in the Hartree–Fock approximation is *larger* than in the Hartree approximation. For spin-up electrons it takes the values 6.00 meV, 6.56 meV, and 5.42 meV, at $k = 0$.

The screening is thus significantly poorer in the HFA than in the HA due to the exchange interaction. We also find that the subbands have a flatter character around $k = 0$ in the Hartree–Fock approximation than in the Hartree approximation. As a result of the Zeeman term and the exchange interaction, the occupation of the spin-up and spin-down electron states is no longer equal for finite magnetic fields. This is especially apparent when we consider figure 1, where we show the effective g-factor calculated from the Hartree–Fock single-particle energies as a function of the momentum k and the subband index, for the three lowest subbands. We define the effective g-factor as

$$g_n^k = (\epsilon_{k,n,+1}^{HF} - \epsilon_{k,n,-1}^{HF})/(g\mu_B B). \tag{9}$$

Thus, for non-interacting electrons we would have $g_n^k = 1$. Starting at the subband $n = 2$, we see that since this subband is close to the Fermi level, there is a large enhancement of the effective g-factor (by one order of magnitude) for the states close to $k = 0$. For larger values of k, subband 2 is further away from the chemical potential, the exchange splitting of the subbands is weaker, and hence the effective g-factor is reduced. However, we find that the g-factor does not decrease monotonically, but is in fact an oscillating function of the momentum k with decreasing amplitude for increasing longitudinal momentum. The same behaviour can be seen for the g-factor associated with the subband $n = 1$, which is *out of phase* with the oscillations of the g-factor associated with subband $n = 2$. The subband $n = 0$ also shows oscillations, but with a larger period in k. We believe that these oscillations are an effect of the confinement of the wire. The subband $n = 0$ has a larger Fermi wave-vector than subband $n = 1$, and this could possibly explain the period of the oscillations of the g-factor being larger for subband $n = 1$ than for subband $n = 0$. The Fermi wave-vectors for the lowest spin subband ($n = 0$) are $k_{F,0,1} = 2.3 \times 10^5$ cm^{-1} and $k_{F,0,-1} = 2.3 \times 10^5$ cm^{-1}, and for the next spin subband ($n = 1$) $k_{F,1,1} = 1.6 \times 10^5$ cm^{-1} and $k_{F,1,-1} = 1.6 \times 10^5$ cm^{-1}. In comparison, the period of the oscillation in g_0^k is around 2.5×10^5 cm^{-1}, and the period of the oscillation in g_1^k is around 1.2×10^5 cm^{-1}. There is no Fermi wave-vector associated with subband 2, and the period of the oscillation in g_2^k is in between the periods of the oscillations in g_0^k and g_1^k. For this subband, the amplitudes of the oscillations in the g-factor are so large that it creates states that have the spins inverted [30, 31]; that is, the effective g-factor is *negative* for some regions of longitudinal wave-vectors. However, one should be cautious about the cases in which the g-factor changes its sign due to the electron–electron interaction. It could be that we are in a regime where the Hartree–Fock approximation is unstable.

Finally, for the case where $B = 2.00$ T, we show, in figure 2, the spin-density excitations calculated within the H-RPA (upper panel) and the HF-RPA (lower panel). In the plot of the spin-density excitations we have given the excitations a phenomenological Lorentzian broadening of 0.05 meV. As mentioned in the introduction, the spin-density excitation spectra in the H-RPA are given by the Hartree single-particle excitations. These excitation energies are thus lowered with respect to the effective subband separation $\overline{h}\Omega$, due to the screening of the external potential. Since in GaAs the g-factor is negative, the Hartree eigenenergies satisfy $\epsilon_{n,k,1}^H < \epsilon_{n,k,-1}^H$. Therefore, the excitation energies for the spin-flip χ_{σ_-}-mode are larger than the excitation energies for the χ_{σ_+}-mode as seen in the upper part of figure 2. The spectrum is broadened due to the k-dependent Hartree subband separation. In the lower part of figure 2, we see the spin-density excitations including the exchange interaction (calculated in the HF-RPA). First, we observe that these peaks have a more collective character than the spectra in the H-RPA, since the peaks are sharper. Second, the energy of these peaks is lower than what the H-RPA predicts, even though the screening is poorer in the Hartree–Fock approximation than in the Hartree approximation. Therefore,

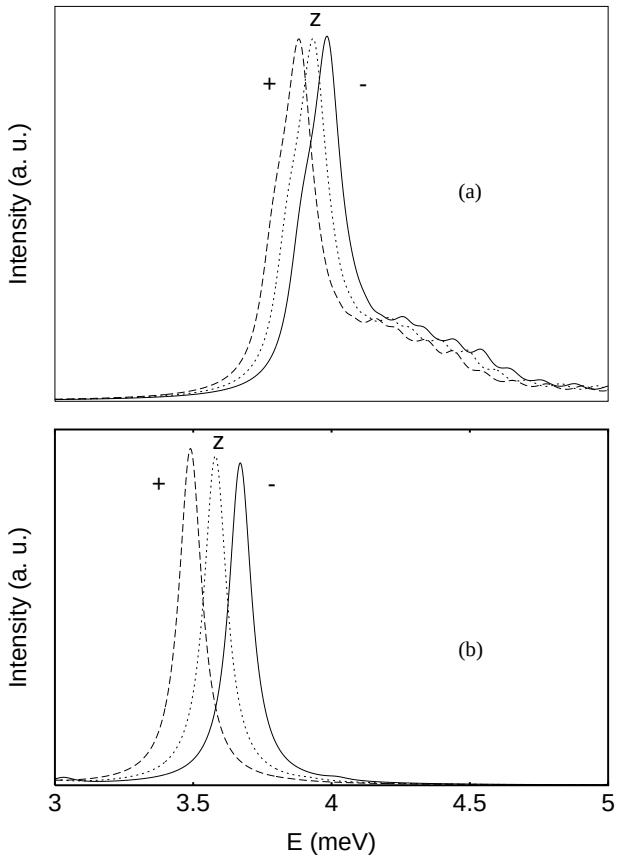

Figure 2. The intensity of spin-density and spin-flip excitations for $B = 2.00$ T as a function of the excitation energy calculated using the H-RPA (a) and calculated using the HF-RPA (b). The label $i = +, -, z$ denotes the three different spin-density modes, $-\mathrm{Im}\,\chi_i$. The other system parameters are as for figure 1.

the vertex corrections are strong and important. We also see that the splitting of the three spin-density modes z, $+$, and $-$, is larger in the HFA than in the HA, which is an effect of the enhancement of the g-factor in the single-particle Hartree–Fock energies. The splitting of the spin-density modes corresponds to an effective g-factor of 1.8. This is seen to be reasonable when we compare with the values of the g-factor in figure 1. The splitting of the excited modes takes an average value of the g-factor over the occupied longitudinal momentum k.

Second, we discuss the case of a magnetic field $B = 1.75$ T ($l_c = 194$ Å). The resulting effective subband separation is $\bar{h}\Omega = 6.54$ meV. In the Hartree approximation, three subbands are occupied, with only a very small occupation of the third subband. The energy separation between subband $n = 0$ and $n = 1$ is 3.47 meV, it is 3.52 meV between subband $n = 1$ and $n = 2$, and it is 3.50 meV between subband $n = 2$ and $n = 3$. Since the third subband is very close to the Fermi energy, the exchange interaction has a drastic effect in this case. We show in figure 3 the Hartree–Fock eigenenergies as a function of the longitudinal momentum k. States with spin up ($\sigma = 1$) are denoted by $+$ and states with spin down ($\sigma = -1$) are denoted by $*$. We see that for spin-up electrons three subbands

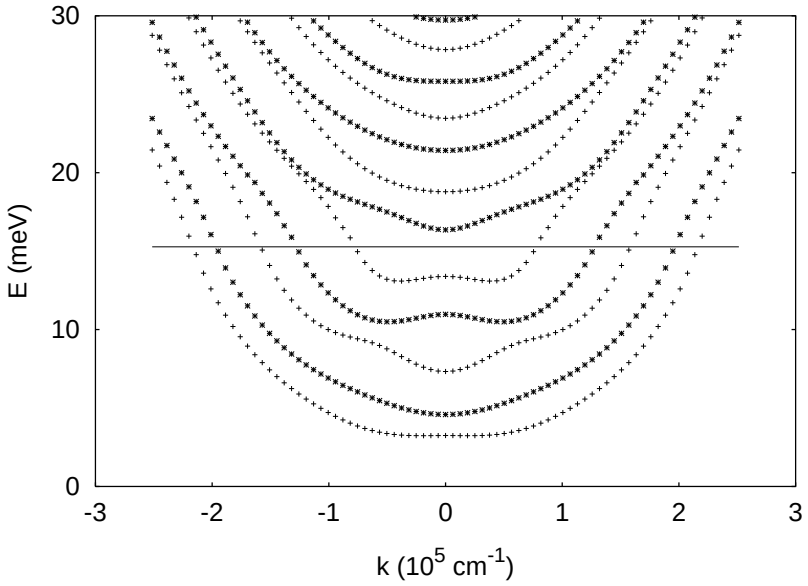

Figure 3. Hartree–Fock eigenenergies for $B = 1.75$ T as a function of the longitudinal momentum. Spin-up states ($\sigma = 1$) are denoted by $+$ and spin-down states ($\sigma = -1$) are denoted by $*$. The other system parameters are as for figure 1.

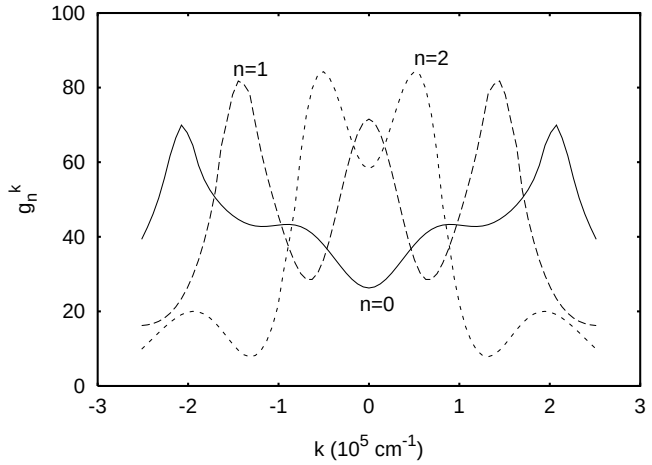

Figure 4. The effective g-factor calculated in the Hartree–Fock approximation for $B = 1.75$ T as a function of the longitudinal momentum. The other system parameters are as for figure 1.

are occupied, and that only two subbands are occupied for spin-down electrons. There is an almost two-orders-of-magnitude enhancement of the g-factor as shown in figure 4. The enhancement is largest for the subband $n = 2$ which is close to the Fermi energy. We see also here oscillations in the enhancement of the g-factor as a function of the longitudinal momentum k for the different subbands.

Within the H-RPA, the spin-density excitation spectra shown in the upper part of figure 5 look qualitatively the same for $B = 1.75$ T as for the case already discussed above ($B = 2.00$ T). We see in figure 5 broad peaks centred around the single-particle

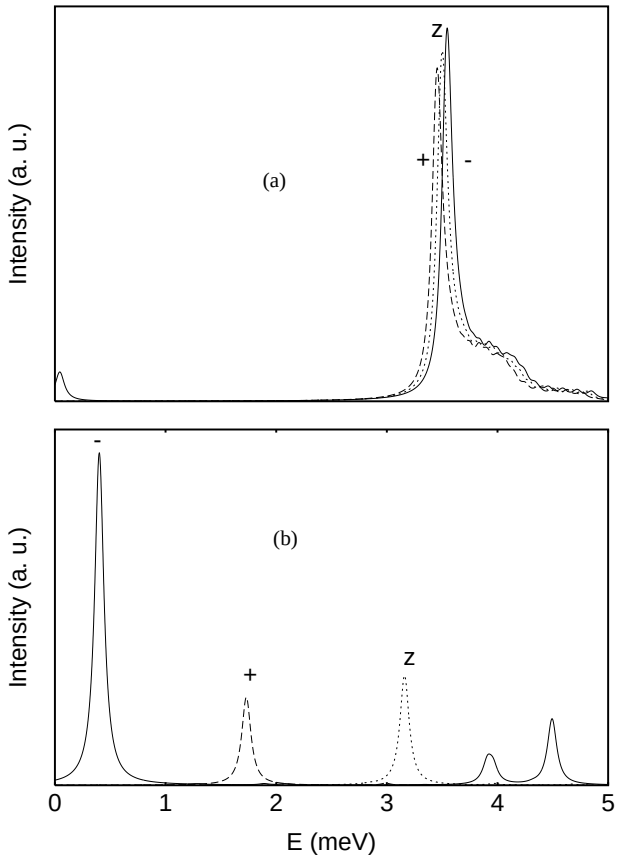

Figure 5. The intensity of spin-density and spin-flip excitations for $B = 1.75$ T as a function of the excitation energy calculated using the H-RPA and calculated using the HF-RPA (b). The label $i = +, -, z$ denotes the three different spin-density modes, $-\mathrm{Im}\,\chi_i$. The other system parameters are as for figure 1.

excitation energy 3.50 meV. In addition, since there is a finite difference in the occupation of spin-up and spin-down electrons in the subband $n = 2$, which is close to the chemical potential, we see a spin-wave mode for low energies due to the intrasubband excitation appearing in the spin-flip mode χ_{σ_-}.

There is a drastic change in the spectra within the HF-RPA shown in the lower part of figure 5 as compared to the calculated H-RPA spin-density excitation spectra. For the spin-density mode χ_{σ_z}, we find one narrow peak which is significantly shifted to lower energies with respect to the Hartree–Fock single-particle energies. For the spin-flip mode χ_{σ_+} we also see one narrow peak due to the collective intersubband transition which is considerably red-shifted with respect to the χ_{σ_z}-mode. The difference in energy between the χ_{σ_z}- and χ_{σ_+}-modes corresponds to an effective g-factor of 42 which also here appears as a reasonable average of the effective g-factor of the single-particle states shown in figure 4. Finally, for the χ_{σ_-}-mode, we see three narrow peaks. The lowest-energy peak is the spin-wave mode associated with the energy of the intrasubband spin-flip transition in the subband $n = 2$. This is the strongest peak in the spectra. The energy of the spin-wave mode is 0.4 meV, and is greatly reduced with respect to the single-particle Hartree–Fock energy difference

at $k = 0$, $\epsilon_{2,0,1} - \epsilon_{2,0,-1} = 3.0$ meV, due to the vertex corrections. There are also two higher-energy peaks for the χ_{σ_-}-modes. We interpret these modes as arising from spin-flip excitations from subband $n = 0$ to subband $n = 1$ and from spin-flip excitations from subband $n = 1$ to subband $n = 2$. In the case of $B = 2.00$ T these two transitions showed up in the spectra as only a single collective peak in figure 2. In the case here ($B = 1.75$ T) the Hartree–Fock single-particle energies for these two possible transitions differ so much due to the complicated strong enhancement of the g-factor that the vertex correction is not strong enough to produce just one collective peak, and as a result two peaks are seen.

4. Concluding remarks

In the calculation of the ground-state Hartree–Fock wave-function, we have seen how the effective g-factor is enhanced when the chemical potential is aligned with a subband energy. For the given quantum wire parameters the enhancement of the g-factor may be by almost two orders of magnitude. It should be noted that the large enhancement of the g-factor was also found previously in 2D systems [29–31]. We find that the effective g-factor oscillates with the longitudinal momentum. Vertex corrections are important for the spin- density excitations, since they cause collective peaks that are considerably red-shifted with respect to the single-particle excitation energies. We have shown how the three components of the spin-density excitations split in a magnetic field. The splitting is at its maximum when the enhancement of the g-factor is large, as should be expected. The splitting takes an average of the enhancement of the g-factor for the occupied states.

The Hartree–Fock approximation may give too large an enhancement of the g-factor due to the strong exchange force that is reduced in better approximations where higher-order correlation effects are included. The same is also true for the vertex corrections which tend to be strong. If the external parabolic potential separation is lowered, keeping all other parameters the same as already discussed, the spin-density excitation energy at $B = 0$ T approaches zero at around $\hbar\omega_0 = 4.0$ meV, and the spin-density excitations are overdamped for smaller subband separations. This is an artifact of the HF-RPA [19].

A consequence of a finite magnetic field is that in general the z-component of the spin-density excitations and the charge-density excitations are coupled, as can be seen from equation (7). However, in the present calculation we have considered the dipole intersubband excitations in a parabolic confinement. The generalized Kohn theorem then dictates the intersubband charge-density excitation spectra. Hence a coupling of the charge-density excitation spectra and the z-component of the spin-density excitation spectra cannot be directly seen. For a non-parabolic confinement the generalized Kohn theorem is relaxed, and a coupling between the charge-density excitations and the z-component of the spin-density excitations is possible. For the charge-density excitations small anharmonic terms in addition to a parabolic confinement lead to the appearance of Bernstein modes in the charge-density excitation spectra around the harmonics of the cyclotron frequency $\omega = n\omega_c$ ($n = 2, 3, \ldots$) [33, 34]. Since the z-component of the spin-density excitations is coupled to the charge-density excitations, the Bernstein modes will also influence the spectra of the z-component of the spin-density excitation spectra.

We have in our calculations assumed that the electron motion is strongly quantized in the z-direction, thus ignoring the spatial extent of the wave-function in this direction. It is well known that a reduced dimensionality increases the electron–electron interaction. In an experimental situation the spatial extent of the electron density in the z-direction can be comparable to the spatial extent of the electron density in the y-direction. Therefore, the inclusion of a finite extent of the wave-function can be important in a quantitative

comparison with experiments as shown by Reboredo and Proetto for the charge-density excitations in a quantum wire in zero magnetic field [7]. The effects of the finite thickness in zero magnetic field have also been studied by Steinebach *et al* in a self-consistent 3D model, showing that the thickness can be important for the exchange interaction as well [39].

In an experimental situation one would possibly measure the three different components of the spin-density excitations over a large interval of different magnetic fields. In this case one should see the enhanced splitting of the spin-flip modes each time a subband is being depopulated. We have not attempted in this work to provide a plot of the excitation spectra sampled for many different fields. The reason for this is that for a given magnetic field the Hartree–Fock calculation has to be performed with a high degree of accuracy with many different starting points for the eigenstates in order to find the lowest-energy Hartree–Fock self-consistent solution.

Acknowledgments

This work was supported in part by a NorFa grant, the Icelandic Science Foundation, and the University of Iceland Research Fund.

References

[1] Pinczuk A and Abstreiter G 1989 *Light Scattering in Solids V (Springer Topics in Applied Physics 66)* ed M Cardona and G Güntherodt (Berlin: Springer)
[2] Li Q and Sarma S D 1989 *Phys. Rev.* B **40** 5860
[3] Yu H and Hermanson J C 1990 *Phys. Rev.* B **42** 1496
[4] Li Q P and Sarma S D 1991 *Phys. Rev.* B **43** 11 768
[5] Li Q P, Sarma S D and Joynt R 1992 *Phys. Rev.* B **45** 13 713
[6] Wendler L and Grigoryan V G 1994 *Phys. Rev.* B **49** 13 607
[7] Reboredo F A and Proetto C R 1994 *Phys. Rev.* B **50** 15 174
[8] Hwang E and Sarma S D 1994 *Phys. Rev.* B **50** 17 267
[9] Demel T, Heitmann D, Grambow P and Ploog K 1988 *Appl. Phys. Lett.* **53** 2176
[10] Egeler T, Abstreiter G, Weinmann G, Demel T, Heitmann D, Grambow P and Schlapp W 1990 *Phys. Rev. Lett.* **65** 1804
[11] Demel T, Heitmann D, Grambow P and Ploog K 1991 *Phys. Rev. Lett.* **66** 2657
[12] Goñi A R, Pinczuk A, Weiner J S, Calleja J M, Dennis B S, Pfeiffer L N and West K W 1991 *Phys. Rev. Lett.* **67** 3298
[13] Goñi A R, Pinczuk A, Weiner J S, Dennis B S, Pfeiffer L N and West K W 1993 *Phys. Rev. Lett.* **70** 1151
[14] Schmeller A, Goñi A R, Pinczuk A, Weiner J S, Calleja J M, Dennis B S, Pfeiffer L N and West K W 1994 *Phys. Rev.* B **49** 14 778
[15] Yang S R E and Aers G C 1992 *Phys. Rev.* B **46** 12 456
[16] Pellegrini V, Pinczuk A, Dennis B S, Plaut A S, Pfeiffer L N and West K W 1997 *Phys. Rev. Lett.* **78** 310
[17] Tanatar B 1996 *Physica* B **228** 329
[18] Brataas A, Mal'shukov A G, Gudmundsson V and Chao K A 1996 *J. Phys.: Condens. Matter* **8** L325
[19] Brataas A, Mal'shukov A G, Gudmundsson V and Chao K A 1997 *Phys. Rev.* B **55** 13 161
[20] Longo J P and Kallin C 1993 *Phys. Rev.* B **47** 4429
[21] MacDonald A H, Oji H C A and Girvin S M 1985 *Phys. Rev. Lett.* **40** 2208
[22] Oji H C A and MacDonald A H 1986 *Phys. Rev.* B **33** 3810
[23] Tomonaga S 1950 *Prog. Theor. Phys. (Kyoto)* **5** 544
[24] Mattis D C and Lieb E H 1965 *J. Math. Phys.* **6** 304
[25] Luttinger J M 1963 *J. Math. Phys.* **4** 1154
[26] Haldane F D M 1981 *J. Phys. C: Solid State Phys.* **14** 2585
[27] Luther A and Emery V J 1974 *Phys. Rev. Lett.* **33** 589
[28] Schulz H J 1993 *Phys. Rev. Lett.* **71** 1864
[29] Ando T and Uemura Y 1974 *J. Phys. Soc. Japan* **37** 1044
[30] Hembree C E, Mason B A, Kwiatkowski J T, Furneaux J and Slinkman J A 1993 *Phys. Rev.* B **48** 9162

[31] Gudmundsson V and Palacios J J 1995 *Phys. Rev.* B **52** 11 266
[32] Manolescu A and Gerhardts R R 1995 *Phys. Rev.* B **51** 1703
[33] Gudmundsson V, Brataas A, Grambow P, Meurer B, Kurth T and Heitmann D 1995 *Phys. Rev.* B **55** 17 744
[34] Brataas A, Gudmundsson V, Mal'shukov A G and Chao K A 1996 *J. Phys.: Condens. Matter* **8** 4797
[35] Hamilton D C and McWhorter A L 1969 *Light Scattering Spectra of Solids* ed G B Wright (New York: Springer)
[36] Kallin C and Halperin B I 1984 *Phys. Rev.* B **30** 5655
[37] MacDonald A H 1985 *J. Phys. C: Solid State Phys.* **18** 1003
[38] Kohn W 1961 *Phys. Rev.* **123** 1242
[39] Steinebach C, Schüller C, Biese G, Heitmann D and Eberl K 1997 *Phys. Rev.* B **57** 1703